

Characterization of Bulk to Thin Wall Mechanical Response Transition in Powder Bed AM

Ben Brown¹, Wes Everhart¹, and Joe Dinardo¹

¹Department of Energy's National Security Campus Managed by Honeywell FM&T, Kansas City, MO 64147

REVIEWED

Notice: This manuscript has been authored by Honeywell Federal Manufacturing & Technologies under Contract No.DE-NA-0000622 with the U.S. Department of Energy. The United States Government retains and the publisher, by accepting the article for publication, acknowledges that the United States Government retains a nonexclusive, paid-up, irrevocable, world-wide license to publish or reproduce the published form of this manuscript, or allow others to do so, for United States Government purposes

Abstract

In the development of powder bed AM process parameters, the characterization of mechanical properties is generally performed through relatively large mechanical test samples that represent a bulk response. This provides an accurate representation of mechanical properties for equivalently sized or larger parts. However as feature size is reduced, mechanical properties transition from a standard bulk response to a thin wall response where lower power border scans and surface roughness have a larger effect. This study identifies this threshold between bulk and thin wall for 304L SS on the Selective Laser Melting (SLM) platform and Ti-6Al-4V on the Electron Beam Melting (EBM) platform. A possible method for improving those properties and shifting the transition from bulk to thin wall response to smaller wall thicknesses was investigated. Mechanical testing and fractography was performed on samples to characterize the effect of wall thickness.

Introduction

With the recent advancements in powder bed additive manufacturing (AM) equipment, previously unmanufacturable geometries are now a possibility. Often, the designs most conducive for economically viable AM parts have fine features such as lattice structures or thin walls. The production of these geometries represents a unique problem in the determination of mechanical properties. In this study samples produced by Selective Laser Melting (SLM) and Electron Beam Melting (EBM) were used to investigate the

effect of reducing wall thickness on resultant tensile properties.

The SLM process uses a laser in an inert atmosphere to selectively melt layers of loose metal powder into a solid. EBM also fabricates parts from a bed of loose metal powder, however the energy source is an electron beam necessitating a vacuum environment. Both of these technologies use scan patterns that include unique hatch fill and border scan parameters. Typical hatch fill parameters are developed to achieve dense parts at high build rates and border parameters are developed to smooth the outer surface of the hatch fill scan area resulting in better surface finish. Because of the function of the border scans, they will not necessarily have a sufficient parameter combination to provide adequate interlayer adhesion on their own, resulting in poor mechanical properties. As a part's thickness reduces, an increasingly greater percentage of the cross sectional area is built with the non-structural border parameters.

Though the effect of fine feature geometry may significantly impact part performance, very little work has been done in this area for AM produced parts. Examples of the large bulk specimen used in many standard development practices include use of 10 mm x 10 mm x 7 mm density pillars [4] and the \varnothing 10 mm tensile specimen used by Niendorf et al. [6]. Ahujaa et al. [3] demonstrated an ability to build walls at 100 μ m thick and used these machine parameters to build larger bulk samples. This was accomplished with only single line hatch fill scans and no smoothing contours, resulting in an apparent rough surface finish. Ideally for end use fine feature parts, fully dense and smooth geometries would be produced. Because AM produces a relatively rough surface finish under ideal conditions, it is especially prone to decreased mechanical properties and surface initiated failure. Krauss et al. [5] demonstrated that thin walls can exhibit a very rough surface if not compensated for and that the manufacturability of thin walls is orientation dependent. Song et al. [9] optimized processing parameters to achieve a desired wall thickness based on input energy. Qui et al. [8] produced thin lattice structures that were then mechanically tested in compression. This study demonstrated the relationship of laser parameters on resulting part porosity and geometry. Abele et al. showed how increased porosity leads to a reduction in mechanical properties in large samples and at thin geometries porosity creates a threshold for achieving gastight parts [2]. For comparison to thin wall tensile testing of similar materials with different processing methods, the work of Pardoen et al. [7] showed that the mechanical response of 316L is not sensitive to change in thickness down to 0.63 mm. From these previous studies it can be seen that using a standard set of parameters results in a threshold for mechanical properties when reducing wall thickness. By identifying and characterizing the reasons for this threshold where the response changes, scan patterns can be manipulated to reduce or even eliminate this effect.

Experimental Setup

For this research, a Renishaw AM250 SLM system and an Arcam A2X EBM system were used. The AM250 uses a 1070 nm fiber laser with a maximum output of 200 W and an approximate spot diameter of 70 μ m. The 304L powder used was 15-45 μ m diameter. The Renishaw AM250 uses a point exposure scan pattern where a single point is exposed, the laser is turned off, repositioned, and then the next point is exposed. The next layer

is then exposed in the same way, however the pattern is rotated a specified amount. A diagram of this Standard scan pattern is illustrated in Figure 1.

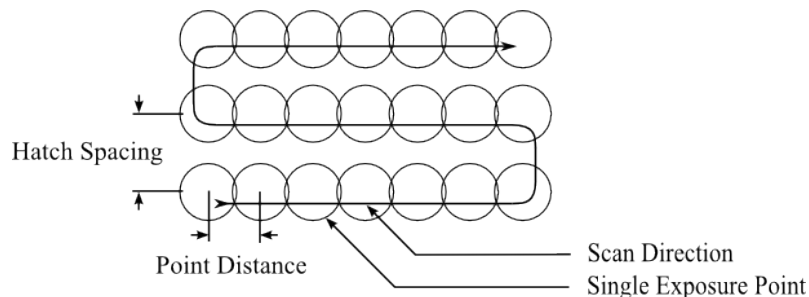


Figure 1: Schematic of the point wise AM250 Hatch Fill Scan Pattern

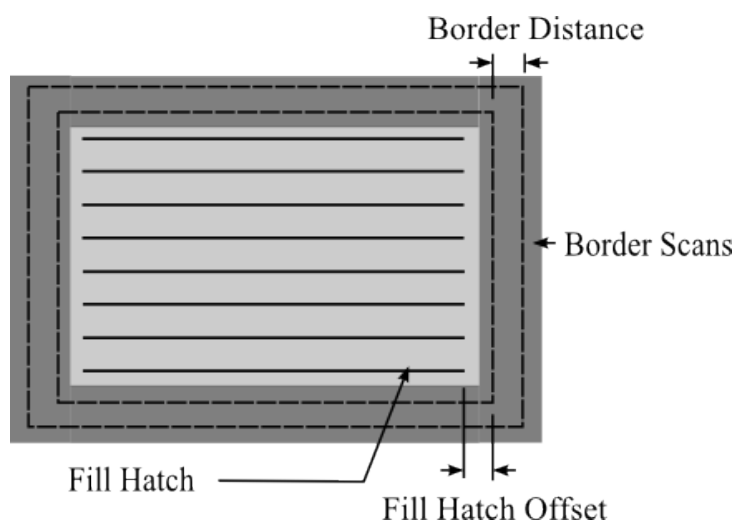


Figure 2: Schematic of the AM250 Border Scan Offsets for one layer the Standard Parameter Set

In addition to the illustrated hatch fill pattern, two border scans are used to smooth the outer profile. A schematic of hatch fill and border scans can be found in Figure 2. A spot compensation is also applied to the outer most border scan. This distance compensates for the width of the laser spot, allowing for a more accurate geometry on the part. With this scan pattern, laser power, point distance, exposure time, and offsets between subsequent hatch fill and border scans are all user defined. Previously developed 304L parameters sets were used for building samples on the AM250. A summary of the differences between hatch fill and border scan parameters can be found in Table 1. The hatch spacing between hatch fill scans was set to $85 \mu\text{m}$, border distance was $40 \mu\text{m}$, and the fill hatch offset was $45 \mu\text{m}$.

Table 1: AM250 Scan Parameters

Machine Parameter	Hatch Fill	Border
Laser Power (watts)	200	150
Point Distance (μm)	85	75
Exposure Time (μsec)	53	100

The Arcam A2X uses a 3000 W electron beam output with an approximate spot size of 200 μm . The vacuum chamber is pumped down to 10^{-4} mbar pressure when building. The Ti-6Al-4V samples built on the A2X used stock parameters and powder 45-100 μm diameter. The scan pattern used by the A2X is an orthogonal hatch for the border followed by a hatch fill scan. While border scans and hatch fill scan utilize separate parameter sets, specific comparison for current and speed are not discussed due to the complexity of parameters and their dependence on part geometry.

Flat samples conforming to ASTM E8 [1] with a gage length of 50.0 mm and gage width of 12.5 mm were produced in the vertical orientation at the varying model thicknesses of 4.0, 3.0, 2.0, 1.0, 0.75, 0.5, and 0.25 mm. Samples were oriented perpendicular relative to the recoating direction of each machine, resulting in a greater stiffness. Each sample was produced in triplicate, removed from the build plate, and mechanically tested per ASTM E8. Due to the rough surface of the samples, the cross sectional area exhibits error. Scanning electron microscopy was performed on fracture surfaces and sample cross sections.

Results and Discussion

The first set of SLM 304L mechanical testing can be found in Figure 3. It should be noted that samples were overbuilt due to lack of spot compensation from the modeled geometries previously listed and that all strength calculations were performed using measured thicknesses. Thickness on Figures 3, 12, and 10 all list the average measured thickness by digital calipers from each set of three samples.

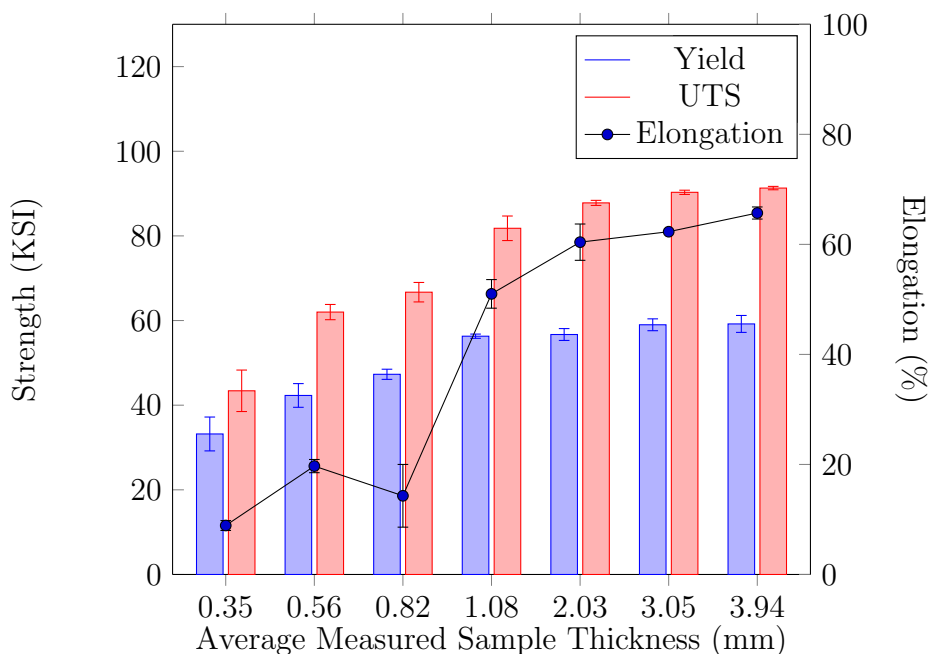


Figure 3: Mechanical Results for SLM 304L Standard Parameters

It can be seen here that for the sample model thicknesses from 4.0 mm down through 2.0 mm, the mechanical response is nearly the identical. These results correspond with

previous testing results from round specimens of roughly the same size and meets the tensile properties typically seen by annealed 304L. Once the model thickness is reduced to 1.0 mm or below, properties begin to significantly reduce and a large drop in elongation to failure is present. From this data, it is apparent that the threshold from bulk to thin wall behavior for this parameter set occurs between a modeled wall thickness of 1.0 mm and 0.75 mm.

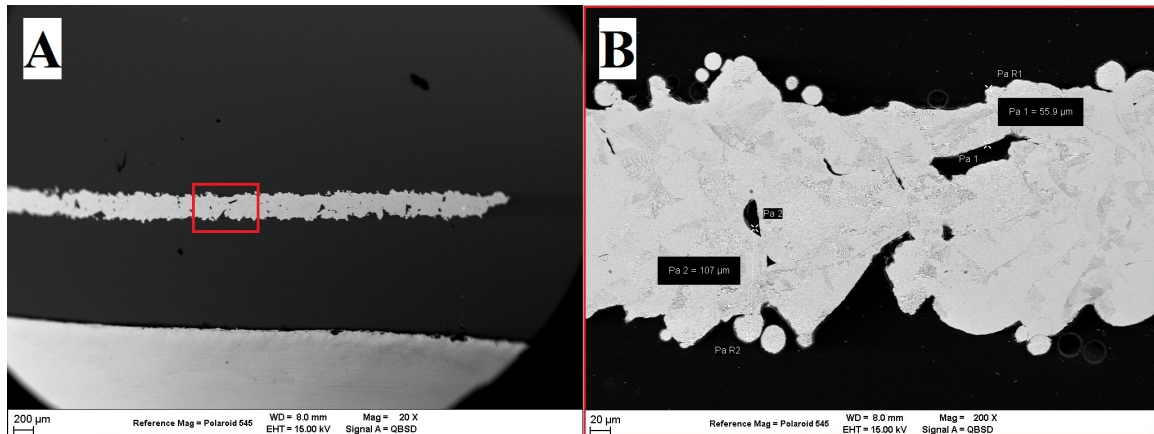


Figure 4: 0.25 mm Sample Built with Standard Parameters Imaged at x25 (A) and x200 (B)

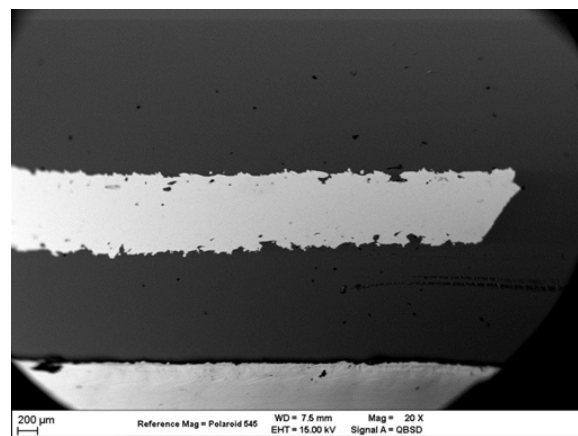


Figure 5: 1.0 mm Sample Built with Standard Parameters Bulk Scan Pattern Imaged at x25

To further investigate the cause of this transition, fractured samples were sectioned longitudinally, mounted, and imaged. The micrographs of the 0.25 mm and 1.0 mm model thickness samples can be found in Figures 4 and 5, respectively. These sectioned images expose multiple regions of reduced cross section and stress concentration, both of which can lead to failure initiation near the surface of the sample. Even with these imperfections, the samples still exhibited a typical ductile failure as indicated by necking in the gauge section and the angled shear plane on the fractured end. Figure 5 shows grouping of internal pores near the surface of the sample. This location corresponds well to the interface between hatch fill and border scans. At a thickness of 0.25 mm nearly 60% of the cross section is border scans. This phenomenon seen in the 1.0 mm sample is

likely still in effect in the 0.25 mm model thickness, but any transition is hard to discern. Figure 4 shows a high amount of surface inconsistencies and voids in the 0.25 mm model thickness sample. The gross failure in this sample is likely due to the high percentage of border parameters resulting in low interlayer strength, sub surface porosity, and stress risers resulting from surface roughness.

When the images of the fractured thin wall samples are compared to a micrograph of a 12.5 mm cube in Figure 6, it can be seen that a bulk sample in the as built condition has subsurface porosity located at the hatch fill and border scan interface, but at much lower frequency. Overall, results indicate that although these border scan parameters result in a relatively uniform surface finish, as they begin to dominate the cross section of a part, tensile properties are affected.



Figure 6: 304L Bulk Sample Imaged at x300

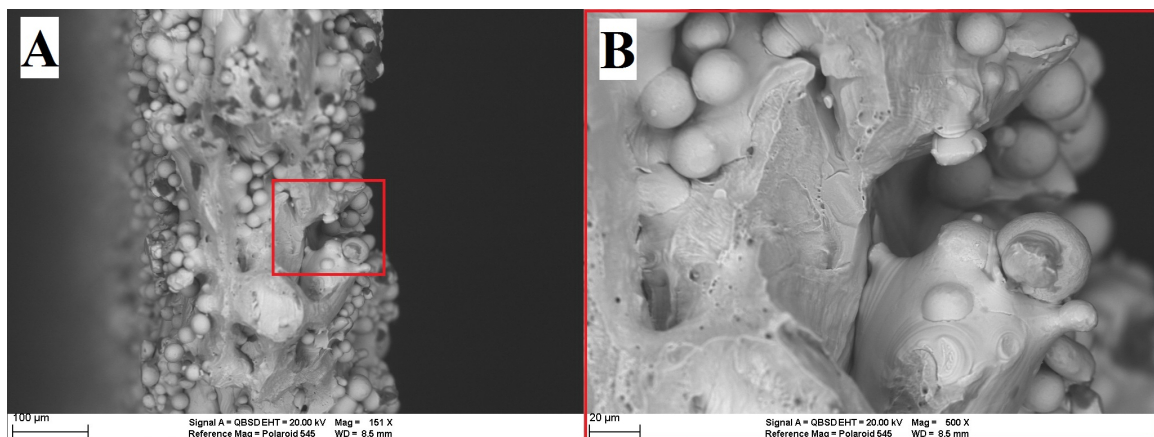


Figure 7: Fractography of 0.25 mm Sample Imaged at x151 (A) and x500 (B) Showing Surface Inconsistencies

Fractography was performed on the samples and results for the 0.25 mm model thickness and the 1.0 mm model thickness samples. Figure 7 reveals several points of reduced

cross section and partially melted particles within the 0.25 mm model thickness sample. Some localized regions of ductile fractures were found as seen in Figure 8, however the fracture surface was predominantly a shear lip. For the 1.0 mm model thickness sample in Figure 9, analysis reveals a much different surface morphology. Predominant regions of ductile fracture with a shear lip shown in Image C. Collections of large pores around the surface as seen in the cross sectioned images are present and were measured to be approximately 20 μm in size.

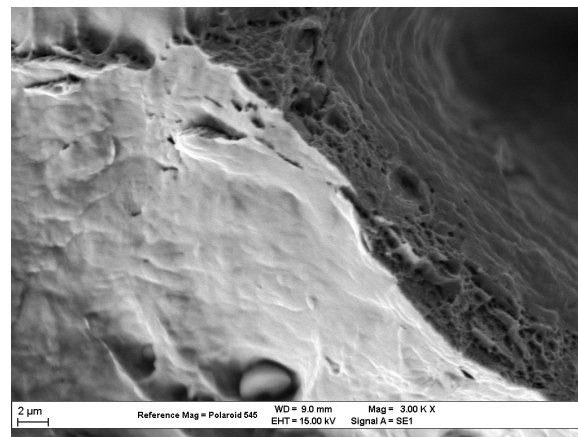


Figure 8: Fractography of 0.25 mm Sample Imaged at x3000 Showing Microvoid Coalescence and Shear Failure

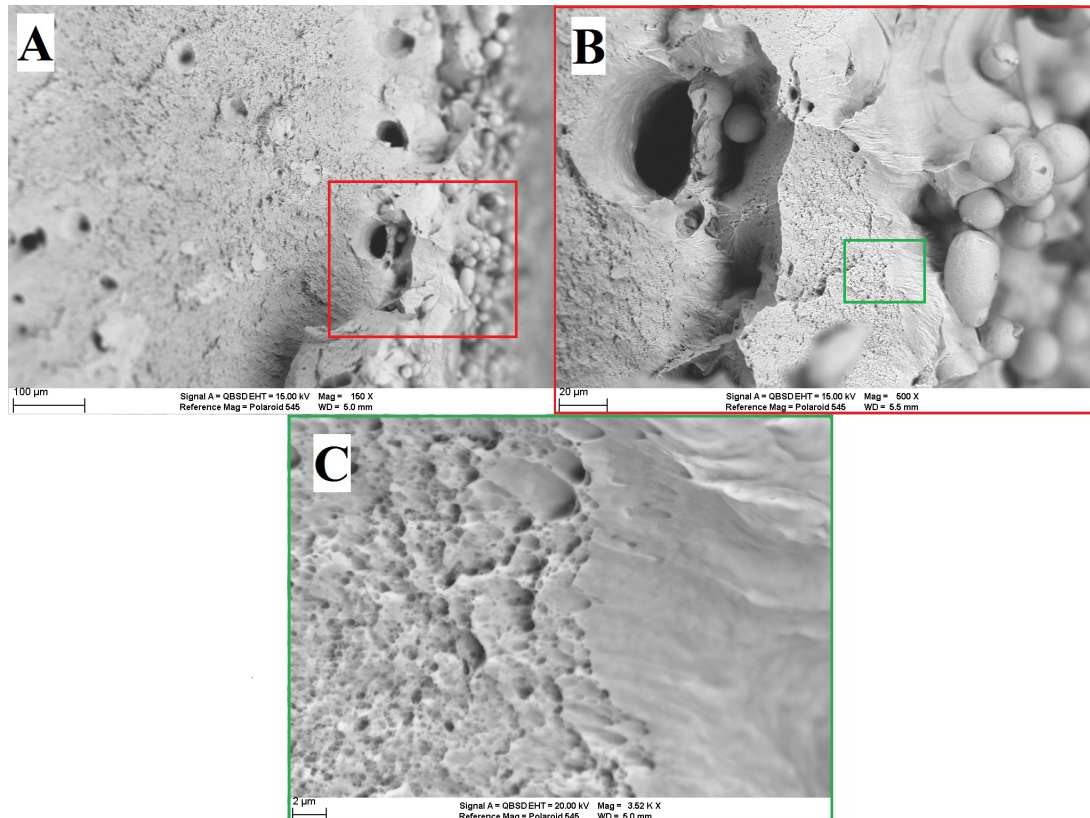


Figure 9: Fractography of 1.0 mm Sample Imaged at x150 (A) and x500 (B) Showing Subsurface Pores, and x3520 (C) Showing Shear Voids

The results for the EBM Ti-6Al-4V samples can be found in Figure 10. From these results it can be seen the the samples above 2.0 mm model thickness all preform the same. Below 2.0 mm model thickness strength begins to reduce and there is a drop in elongation at break from approximately 6% to 2%. The smallest three sample sets, with models at 0.25, 0.50, and 0.75 mm model thickness built at averages of 0.78, 0.79 and 0.81 mm, respectively, showing that the minimum feature size for this combination of machine and material is approximately 0.8 mm. Similar to the SLM 304L, this material exhibits a reduction of tensile properties below a critical size due to reduced effectiveness of the processing parameters.

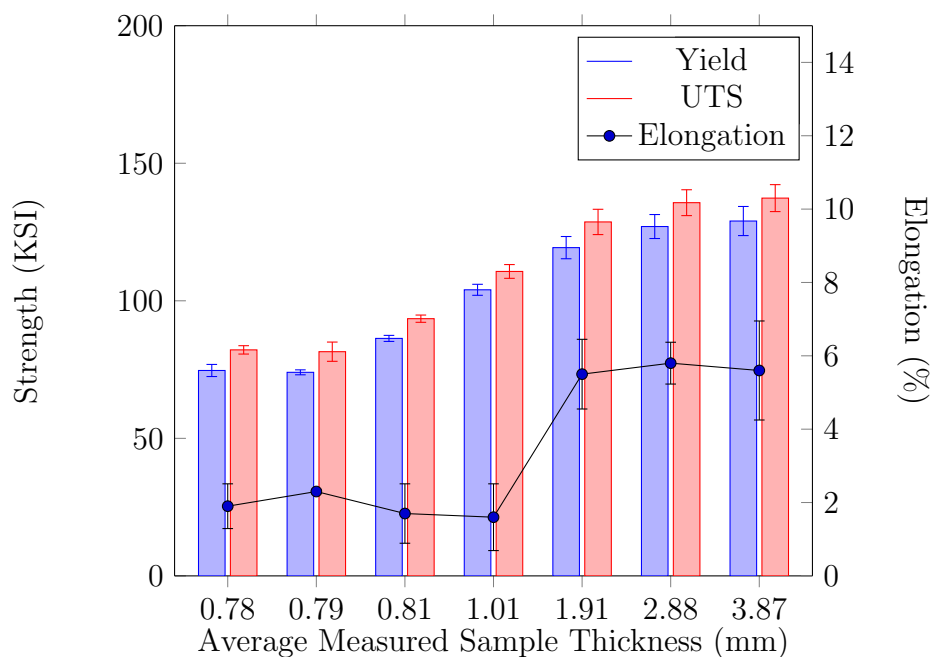


Figure 10: Mechanical Results for EBM Ti-6Al-4V Standard Parameters

In order to compensate for the thin wall effect seen in the SLM 304L standard scan pattern discussed previously, modifications were made. The ratio of hatch fill area to border scan area was increased by reducing the fill hatch offset to 0 μm and reducing the number of border passes from 2 to 1 (Figure 11). Results of the mechanical testing for the compensated parameter set can be found in Figure 12. It can be seen that although strength is not improved, the threshold of thin wall to bulk has shifted from the 1.0 mm to 0.75 mm model thickness range down to the 0.5 mm to 0.25 mm model thickness range, as indicated by the shift in the drop off of elongation at break. The 0.25 mm and 1.0 mm cross section sample images for the compensated parameter set can be found in Figures 13 and 14, respectively. Investigation of the cross sectioned samples reveals an almost total elimination of the large surface porosity seen with the standard parameter set. The sample thickness is also more consistent, resulting in a reduction of stress concentration points. This agrees with the mechanical test results showing improved elongation to failure.

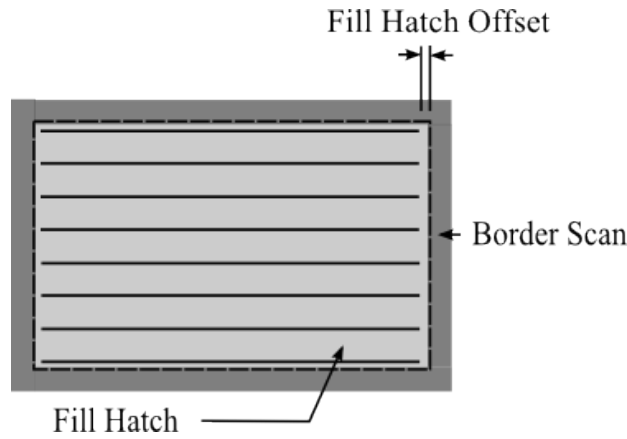


Figure 11: Schematic of Compensated AM250 Border Offsets

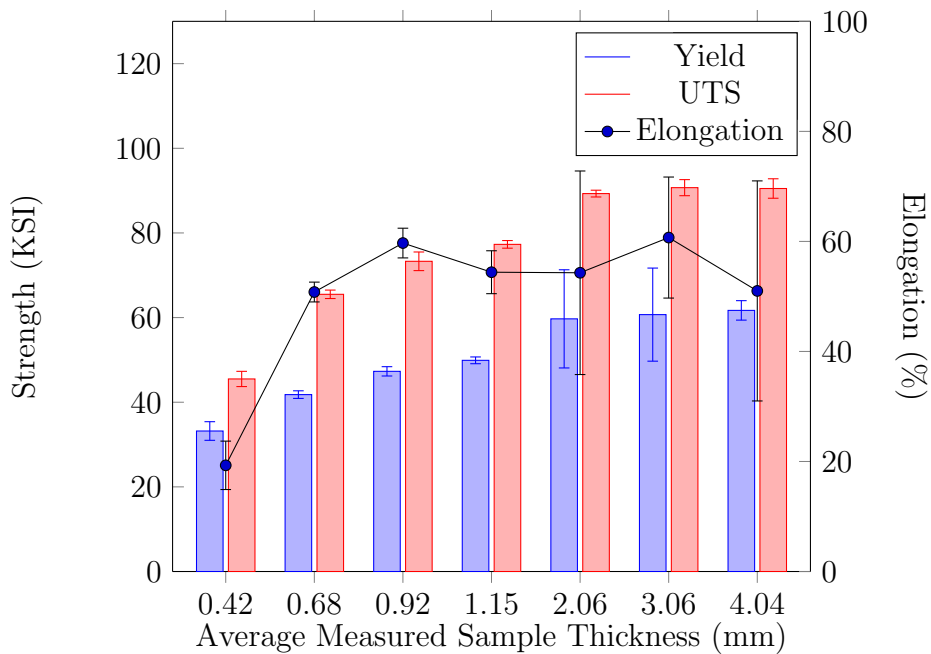


Figure 12: Mechanical Results for SLM 304L Compensated Parameters

Fractography analysis was performed on the samples produced with the compensated scan pattern. The 0.25 mm and 1.0 mm model thickness fracture images are found in Figures 16 and 15, respectively. Analysis of the 0.25 mm model thickness sample reveals a more uniform cross section with much larger regions of ductile failure than in the standard parameter set samples. Unmelted powder is still seen, however it is limited to only the surface of the sample. Investigation of the 1.0 mm model thickness sample reveals that previously seen sub surface porosity is still present, although the pore size has been reduced to approximately 10 μm .

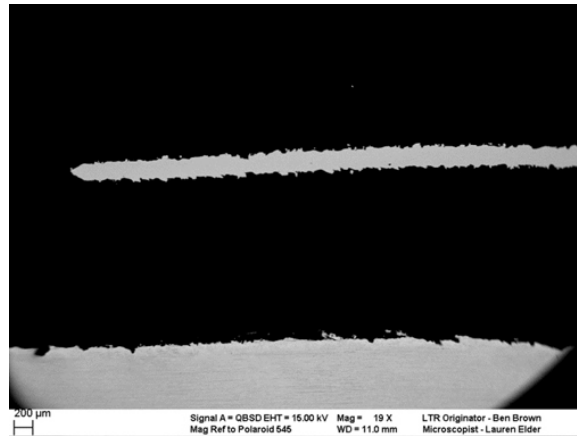


Figure 13: 0.25 mm Sample Built with Compensated Scan Pattern Imaged at x25

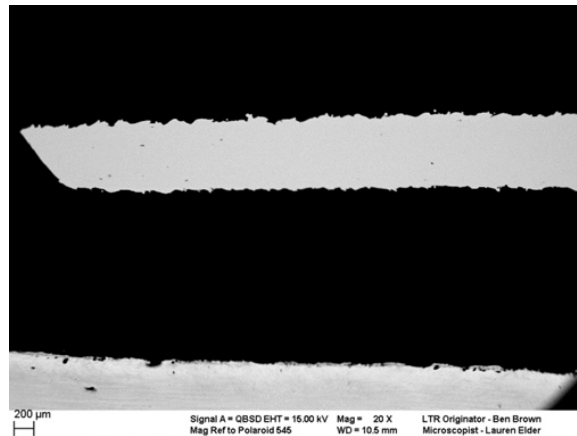


Figure 14: 1.0 mm Sample Built with Compensated Scan Pattern Imaged at x25

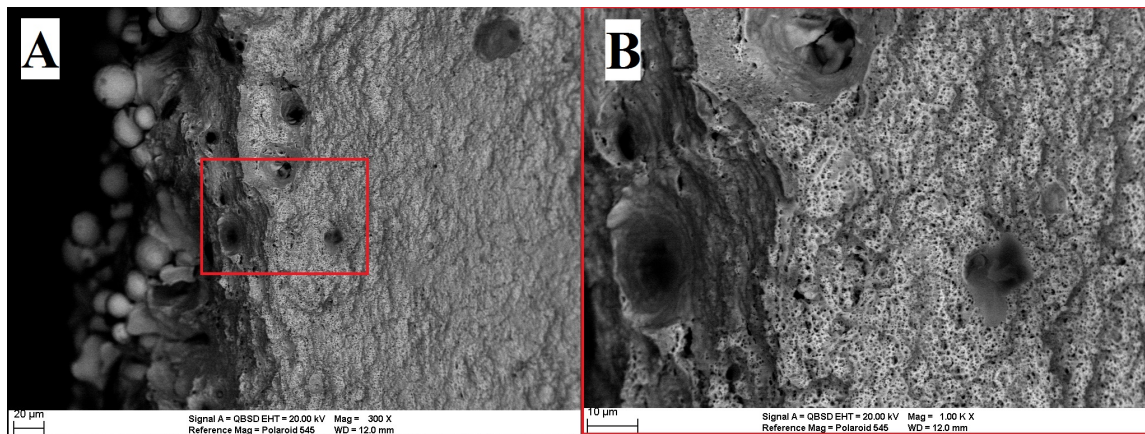


Figure 15: Fractography of 1.0 mm Sample with Compensated Scan Pattern Imaged at x300 (A) and x1000 (B) Showing Sub Surface Pores

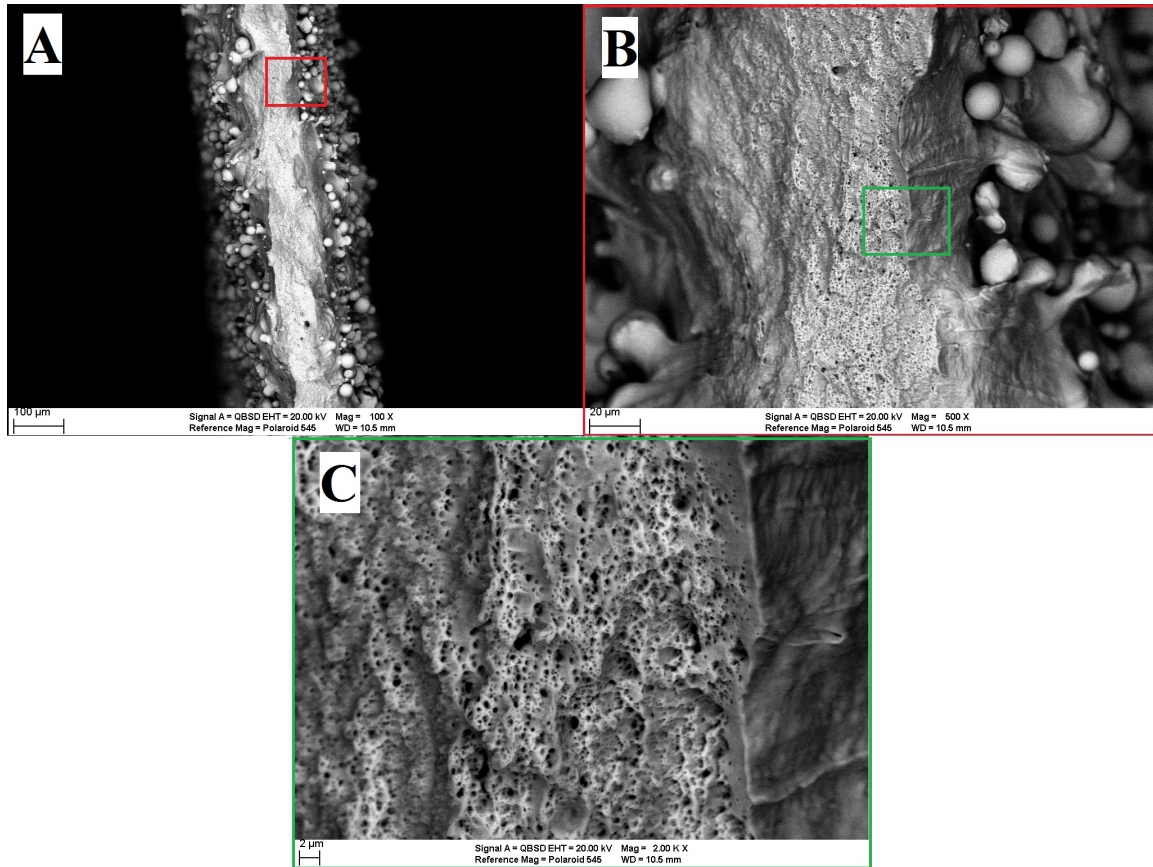


Figure 16: Fractography of 0.25 mm Sample with Compensated Scan Pattern at x100 (A), x500 (B), and x2000 (C) Showing Ductile Failure

Conclusion

In this study, the effect of reducing wall thickness of tensile specimens was analyzed for 304L samples built on the SLM platform and Ti-6Al-4V samples built on the EBM platform. It was seen that by building with a parameter set based on samples representing a bulk response, mechanical properties begin to reduce once a wall thickness threshold is reached. By compensating the scan pattern to increase the area of hatch fill, a more uniform sample cross section with reduced subsurface porosity has been achieved, resulting in a shift of the threshold to a smaller thickness. However, even with a scan pattern optimized for producing thin wall geometry, a reduction in mechanical properties was still seen in parts produced with greatly different materials by the SLM and EBM powder bed processes. This implies that the reduction in tensile properties is a generic response to the reduction of wall thickness in AM parts. Based on cross section micrographs and fractography, it appears that surface roughness and inconsistencies could be the root of this tensile property reduction. Further work needs to be conducted to conclude if this effect is caused by the rough surface finish resulting in stress risers and surface initiated failure.

Acknowledgments

The Authors would like to acknowledge the assistance provided for this research by AM equipment technicians Kevin Davis and Justin Tannehill, as well as microscopists Lauren Elder and Brandon Cox.

All data prepared, analyzed and presented has been developed in a specific context of work and was prepared for internal evaluation and use pursuant to that work authorized under the referenced contract. Reference herein to any specific commercial product, process or service by trade name, trademark, manufacturer, or otherwise, does not necessarily constitute or imply its endorsement, recommendation, or favoring by the United States Government, any agency thereof or Honeywell Federal Manufacturing & Technologies, LLC.

This presentation has been authored by Honeywell Federal Manufacturing & Technologies under Contract No. DE-NA0000622 with the U.S. Department of Energy. The United States Government retains and the publisher, by accepting the article for publication, acknowledges that the United States Government retains a nonexclusive, paid up, irrevocable, world-wide license to publish or reproduce the published form of this manuscript, or allow others to do so, for the United States Government purposes.

References

- [1] ASTM E8 / E8M 15a Standard Test Methods for Tension Testing of Metallic Materials. *ASTM International*, West Conshohocken, PA, 2015.
- [2] Eberhard Abele, Hanns A. Stoffregen, Michael Kniepkamp, Sebastian Lang, and Manfred Hampe. Selective laser melting for manufacturing of thin-walled porous elements. *Journal of Materials Processing Technology*, 215(2015):114–122.
- [3] Bhrihu Ahuja, Adam Schaub, Michael Karg, Michael Lechneb, Marion Merklein, and Michael Schmidt. Developing lbn process parameters for ti-6al-4v thin wall structures and determining the corresponding mechanical characteristics. *Physics Procedia*, 56(2014):90–98.
- [4] Chandrika Kamath, Bassem El-dasher, Gilbert F. Gallegos, Wayne E., King, and Aaron Sisto. Density of additively-manufactured, 316l ss parts using laser powder-bed fusion at powers up to 400 w. *The International Journal of Advanced Manufacturing Technology*, 74:65–78.
- [5] H. Krauss and M. F. Zaeh. Investigations on manufacturability and process reliability of selective laser melting. *Physics Procedia*, 41(2013):815–822.
- [6] Thomas Niendorf, Stefan Leuders, Andre Riemer, Hans Albert Richard, Thomas Trster, and Schwarze Dieter. Highly anisotropic steel processed by selective laser melting. *Metallurgical and Materials Transactions B*, 44(4):794–796.

- [7] T. Pardoen, F. Hacheza, B. Marchionia, P.H. Blythb, and A.G. Atkinsb. Mode 1 fracture of sheet metal. *Journal of the Mechanics and Physics of Solids*, 52(2004):423–452.
- [8] Chunlei Qiu, Sheng Yue, Nicholas J.E. Adkins, Mark Ward, Hany Hassanin, Peter D. Lee, Philip J. Withers, and Moataz M. Attallah. Influence of processing conditions on strut structure and compressive properties of cellular lattice structures fabricated by selective laser melting. *Materials Science & Engineering A*, 628(2015):188–197.
- [9] Changhui Song, Yongqiang Yang, Yang Liu, Ziyi Luo, and Jia-Kuo Yu. Study on manufacturing of w-cu alloy thin wall parts by selective laser melting. *Int J Adv Manuf Technol*, 78:885–893.